
Federated Class-Incremental Learning with Hierarchical Generative Prototypes

Riccardo Salami* Pietro Buzzega* Matteo Mosconi Mattia Verasani Simone Calderara

AIImageLab - University of Modena and Reggio Emilia, Modena, Italy
 name.surname@unimore.it

Abstract

Federated Learning (FL) aims at unburdening the training of deep models by distributing computation across multiple devices (clients) while safeguarding data privacy. On top of that, Federated Continual Learning (FCL) also accounts for data distribution evolving over time, mirroring the dynamic nature of real-world environments. While previous studies have identified Catastrophic Forgetting and Client Drift as primary causes of performance degradation in FCL, we shed light on the importance of *Incremental Bias* and *Federated Bias*, which cause models to prioritize classes that are recently introduced or locally predominant, respectively. Our proposal constrains both biases in the last layer by efficiently fine-tuning a pre-trained backbone using learnable prompts, resulting in clients that produce less biased representations and more biased classifiers. Therefore, instead of solely relying on parameter aggregation, we leverage generative prototypes to effectively balance the predictions of the global model. Our proposed methodology significantly improves the current State Of The Art across six datasets, each including three different scenarios.

1 Introduction

The traditional paradigm in Deep Learning necessitates accessing large-scale datasets all at once, which hinders scalability and raises significant privacy concerns, especially when sensitive data is involved. Although distributing training across many devices could be an effective solution, there is still no effective mechanism for blending the resulting trained models into a single unified one. Federated Learning (FL) [37] addresses this challenge through a centralized server that coordinates distributed devices, aiming to create a single unified model while minimizing communication costs.

Federated Class-Incremental Learning (FCIL) [52, 7, 56] takes a step further and couples distributed training with Online Learning, tolerating distribution shifts in the data over time. This presents new challenges, as deep models learning online (without relying on old examples) experience severe performance degradation due to Catastrophic Forgetting [35]. In FCIL, the training process unfolds in tasks, each of which shifts the data distribution by introducing new categories. Each task is divided into communication rounds, wherein the local models train on their private data distribution. After local training, each client may transmit information to the orchestrator (server), which creates a global model and redistributes it to all clients. In the literature, some methodologies account for architectural heterogeneity (*i.e.*, heterogeneous FL [5, 19, 15]), while others aim to enhance the performance of local models without necessarily converging to a global one (*i.e.*, personalized FL [4, 32, 38]). Instead, we follow the original FCIL setting as presented in [7], with the goal of training a single global model in a distributed way.

*Equal contribution

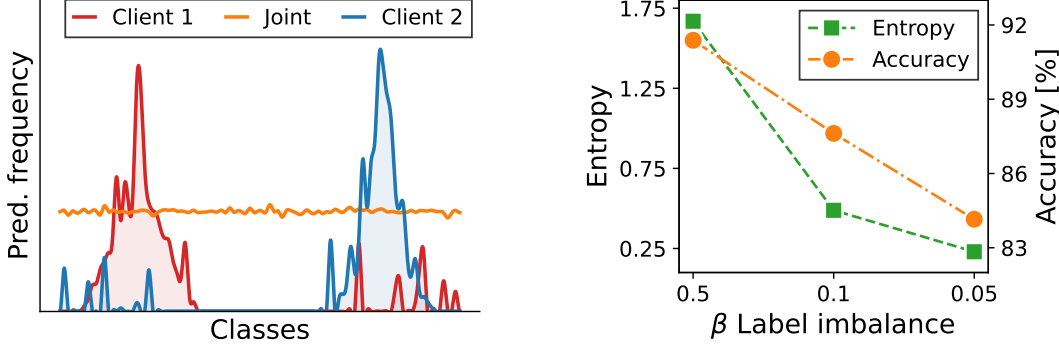


Figure 1: **Federated bias.** Histogram of the clients’ responses computed on the global test set ($\beta = 0.05$). Class indexes have been rearranged for improved visualization (left). The entropy of the response histograms, averaged on all clients, compared with FL performance (right).

When learning on a sequence of tasks, the model struggles the most at differentiating classes from distinct tasks, whereas it works well at separating those within the same one. Albeit one would intuitively link such behavior to Catastrophic Forgetting, it primarily occurs because tasks are learned separately, and some classes are never seen simultaneously [18]. This results in a phenomenon known in the Incremental Learning literature as *bias*, which favors recently introduced classes [51]. We refer to this as Incremental Bias (IB). IB emerges because new classification heads are optimized independently, without concurrent access to previous classes. As a result, gradient updates are disproportionately influenced by the new classes, causing imbalance in the classifier’s output.

The authors of [31] observe a similar tendency in the Federated Learning scenario: since clients train exclusively on their local datasets, they exhibit a bias towards their local label distribution. We refer to this effect as *Federated Bias* (FB). In contrast to the well-known Client Drift [9, 17, 59], which causes misalignment between the clients’ learned *parameters*, Federated Bias affects the clients’ *responses*. Specifically, FB induces clients’ outputs to diverge in different directions, mirroring the patterns of their local label distributions. Also, the strength of FB increases with growing heterogeneity, suggesting a correlation with declining performance (see Section 2). To relieve such an effect, we constrain FB to the last layer by leveraging a frozen pre-trained backbone and efficiently fine-tuning it via prompt learning [26]. Ideally, prompting keeps the clients’ representations close to the pre-training optimum (hence, close to each other), thus minimizing their Federated Bias. In Section 4.3, we experimentally verify that prompting leads to reduced bias in the feature space w.r.t. fine-tuning all parameters. This confines the impact of FB to the last layer, providing the centralized server with less biased representations. On top of that, prompt-based methodologies *i*) have demonstrated SOTA results in Class-Incremental Learning [50, 49, 44] and *ii*) adapt only a small portion of the clients’ parameters, improving communication efficiency in distributed scenarios [57, 29].

The authors of [51, 55, 31] address either IB or FB by fine-tuning the classification layer (where such biases are the most evident) on IID data samples. To meet the privacy requirements of FL, which prohibit transferring real data, we follow recent studies [55, 31] and leverage latent generative replay. Specifically, at each communication round, we alleviate both biases – previously enforced to the last layer by the adopted prompt-based fine-tuning – by rebalancing the global classifier on a dataset of generated representations. In contrast to other approaches relying on prototypes (*i.e.*, the average feature vectors) to regularize clients’ training procedures [45, 10], we propose to compute their covariance matrix and parameterize a Multivariate Gaussian distribution for each class-client combination. This forms a grid of *num_classes* \times *num_clients* *generative prototypes*, which are sampled hierarchically (first by class, then by client) to generate new data points.

Summarizing, this work:

- sheds light on the relation between prompt learning and the aforementioned biases, identifying the latter as the primary cause of performance degradation in FCIL;
- proposes a novel methodology that confines (with prompting) and mitigates (by rebalancing) such biases in the final classification layer;
- provides a comprehensive evaluation of the proposed approach, demonstrating state-of-the-art performance on standard benchmarks while maintaining minimal communication costs.

2 On Federated Bias

This section investigates how Federated Bias in clients’ responses is associated with performance degradation in Federated Learning. All experiments are conducted on the CIFAR-100 [23] dataset, where the data is heterogeneously distributed across 10 clients under the commonly adopted distribution-based label imbalance setting [24, 53].

To effectively show the presence of FB in the local models, we evaluate them at their most biased state: specifically, at the end of the local training, prior to any synchronization with the centralized server. In Figure 1 (left), we show the histogram of the responses given by two randomly selected clients, trained with $\beta = 0.05$, on the global test set. Additionally, we compare them against a model trained conventionally on the global data distribution (referred to as Joint). It can be observed that clients’ predictions are significantly skewed (*i.e.*, biased), mirroring their local label distribution.

To define a quantitative measure for FB, we consider the responses from all clients and compute the average entropy of the histograms of their predictions. Here, low entropy indicates a highly biased model presenting a peaked response distribution, whereas high entropy implies uniformity in the model’s responses and is linked to lower bias. The experiment is repeated for three increasingly challenging label-imbalance settings ($\beta \in \{0.5, 0.1, 0.05\}$). Figure 1 (right) shows the average entropy at the end of the local training compared to the final performance. The two curves are notably similar, suggesting a correlation between Federated Bias and performance deterioration.

3 Methodology

3.1 Problem definition

Federated Class-Incremental Learning [56, 10] tackles a classification problem across C classes, which are introduced sequentially over T incremental tasks. For each task, the data is distributed in a non-IID manner among M clients. Let D^t be the global partition for task t , which is split among the M clients, with D_m^t being the local partition of client m at task t . The training procedure of each task is divided into communication rounds, each consisting of a certain number of epochs. At the end of the local optimization, the clients synchronize with the server by exchanging their learnable parameters. The server aggregates these parameters into a global model and redistributes it to all clients, thus concluding the communication round. Since data from previous tasks is unavailable, client m can only train on its dataset D_m^t during task t . Let f_{θ_m} be the local model of client m , parameterized by θ_m . The local objective is to minimize the loss function \mathcal{L} with respect to the local dataset D_m^t , namely:

$$\underset{\theta_m}{\text{minimize}} \quad \mathbb{E}_{(x,y) \sim D_m^t} \mathcal{L}(f_{\theta_m}(x), y). \quad (1)$$

The goal of the centralized server is to find the optimal set of parameters θ that minimizes the loss function on the entire dataset, without having access to any data point:

$$\underset{\theta}{\text{minimize}} \quad \frac{1}{TM} \sum_{t=1}^T \sum_{m=1}^M \mathbb{E}_{(x,y) \sim D_m^t} \mathcal{L}(f_{\theta}(x), y). \quad (2)$$

3.2 Hierarchical Generative Prototypes

We introduce Hierarchical Generative Prototypes (HGP), which comprises two key components: i) *prompting*, reducing communication costs and constraining Federated and Incremental biases within the classifier; ii) *classifier rebalancing*, addressing these biases on the server side. We report the pseudo-code algorithm in the supplementary material.

Prompting. Differently from other prompt-based CL approaches, which rely on a *pool* of task-generic [50] or task-specific [44, 49] prompts, we propose learning a *single* prompt shared across all tasks. This eliminates the need for prompt selection – which requires an additional forward pass – significantly accelerating both training and inference. Specifically, we instantiate two learnable vectors, P_k and P_v , for each of the first 5 transformer blocks, obtaining the prompt $\mathcal{P} = \{P_k^j, P_v^j \mid j \in 1, \dots, 5\}$. Following prefix-tuning [26], P_k^j and P_v^j are respectively prepended to the keys and values of the j^{th} Multi-head Self Attention layer and optimized jointly to minimize the loss function.

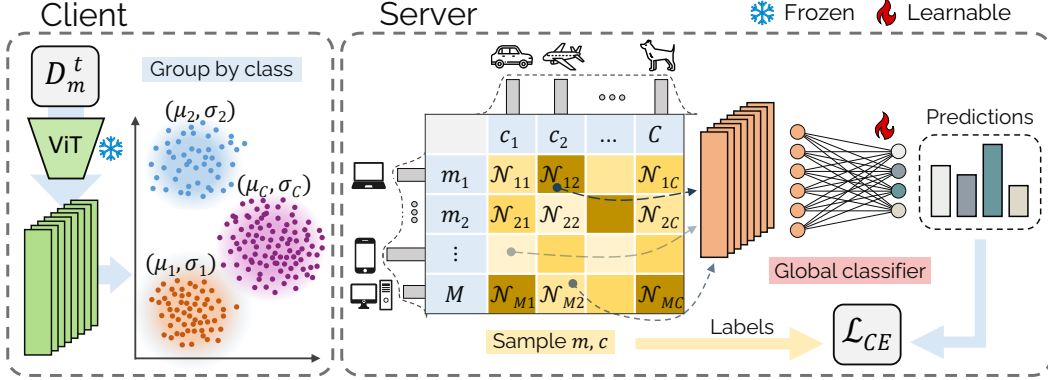


Figure 2: Classifier Rebalancing procedure through hierarchical sampling.

After training on the local data distribution, each client sends its learnable parameters (consisting of prompt and classification head) to the server. Then, given $|D^t| = \sum_{m=1}^M |D_m^t|$, where $|\cdot|$ represents the cardinality of a set, the server aggregates the parameters as:

$$\theta^t = \frac{1}{|D^t|} \sum_{m=1}^M |D_m^t| \theta_m^t. \quad (3)$$

Here, $\theta_m^t = \{\mathcal{P}_m, W_m^t\}$ indicate the learnable parameters of client m during task t (comprising of prompt \mathcal{P}_m and classification head W_m^t).

Classifier Rebalancing. To mitigate biases in the classification head, we employ a rebalancing procedure on the server side. Specifically, we retrain the final classification layer using data entries sampled from *generative prototypes*.

The procedure starts with each client m approximating the distribution of the features h related to class c using a multivariate Gaussian $\mathcal{N}_{m,c}(\mu_{m,c}, \Sigma_{m,c})$, where $\mu_{m,c}$ is the mean and $\Sigma_{m,c}$ the covariance matrix of the feature vectors produced by its local examples belonging to class c (see Figure 2, Client). Since other studies denote $\mu_{m,c}$ as the prototype for client m and class c , we refer to $\mathcal{N}_{m,c}$ as a generative prototype, given its capability to synthesize new samples. By repeating this process across all classes and clients, we produce $M \times C$ prototypes, which need to be combined into a single generative model that best approximates the global data distribution.

For a given class c , the server receives M generative prototypes, one from each client, and seeks to identify the single distribution that best aligns with all of them. To this aim, we take the distribution that minimizes the Jensen-Shannon Divergence (JSD) [28]. Considering multiple distributions $\mathcal{Q} = \{Q_1, \dots, Q_M\}$, with importance weights $\Pi = \{\pi_1, \dots, \pi_M\}$, their JSD is defined as:

$$\text{JSD}_{\Pi}(\mathcal{Q}) = \sum_{m=1}^M \pi_m D_{\text{KL}}(Q_m || G), \quad G = \sum_{m=1}^M \pi_m Q_m, \quad (4)$$

where D_{KL} is the Kullback-Liebler divergence.

Therefore, our objective is to find a global distribution \tilde{Q}_c for the class c that optimizes:

$$\underset{\tilde{Q}_c}{\text{minimize}} \quad \sum_{m=1}^M \pi_{m,c} D_{\text{KL}}(\tilde{Q}_c || G). \quad (5)$$

Notably, the optimal solution to this problem is to set \tilde{Q}_c equal to the distribution G . Since, in our case, all distributions $\{Q_1, \dots, Q_M\}$ are Gaussians, the closest distribution G is precisely defined as a Gaussian Mixture Model (GMM). Following a common practice in Federated Learning [45, 37], we assign the importance weights $\{\pi_{1,c}, \dots, \pi_{M,c}\}$ to the generative prototypes based on the number of samples from class c observed by client m .

By solving Equation 5 for all classes, we result in C GMMs, $\{\tilde{Q}_1, \dots, \tilde{Q}_C\}$, one for each class. To obtain a single generative model, we further combine them by following a similar reasoning to the one of Equation 5. This time, we consider those C class-specific GMMs as the initial distributions in Equation 4, which leads us to define the global generative model \tilde{Q} over all classes:

$$\tilde{Q} = \sum_{c=1}^C \omega_c \tilde{Q}_c, \quad \tilde{Q}_c \triangleq \sum_{m=1}^M \pi_{m,c} \mathcal{N}_{m,c}(\mu_{m,c}, \Sigma_{m,c}), \quad (6)$$

where the class-specific weights $\{\omega_1, \dots, \omega_C\}$ are set to the normalized number of samples for each class. According to Equation 5, \tilde{Q} is the distribution that most closely aligns with all class-specific GMMs: consequently, it also provides the closest match to all the initial Gaussians across every class-client combination.

When it comes to sampling from \tilde{Q} , we recall that the standard GMM sampling process consists of two steps: first, selecting a Gaussian, and then sampling from it. Expanding on this framework, we introduce an additional step, which is used to select the class-specific GMM \tilde{Q}_c from the global distribution \tilde{Q} . Specifically, as illustrated in Figure 2 (Server), our hierarchical sampling strategy draws: *i*) the class-specific GMM index (c) from a Multinomial distribution on the class weights $\{\omega_1, \dots, \omega_C\}$; *ii*) the client-specific Gaussian index (m) from a Multinomial distribution on the class-client weights $\{\pi_{1,c}, \dots, \pi_{M,c}\}$; *iii*) the synthetic feature \hat{h} from the generative prototype $\mathcal{N}_{m,c}$.

At the conclusion of each communication round, the server *i*) generates a synthetic dataset \hat{D} by sampling from \tilde{Q} ; *ii*) aggregates the clients' learnable parameters θ_m^t according to Equation 3; *iii*) rebalances the global classifier G , parameterized by W . This latter step is achieved by minimizing the Cross-Entropy (CE) loss w.r.t. \hat{D} :

$$\underset{W}{\text{minimize}} \mathbb{E}_{(\hat{h}, c) \sim \hat{D}} \mathcal{L}_{\text{CE}}(G_W(\hat{h}), c). \quad (7)$$

Finally, the server redistributes the updated classifier along with the aggregated prompt to the clients, enabling them to start the next training round. We refer the reader to the supplementary material for a detailed analysis of the computational complexity of our approach.

4 Experiments

In this section, we assess the effectiveness of the proposed method, comparing it with the current State of The Art in Federated Class-Incremental Learning.

4.1 Settings

Datasets. Following [43], we evaluated the proposed method on *six* diverse datasets, spanning both in-distribution and out-of-distribution domains: *CIFAR-100* [23], *ImageNet-R* [12], *ImageNet-A* [13], *EuroSAT* [11], *Cars-196* [22], and *CUB-200* [47]. All datasets are partitioned into 10 incremental tasks, except for *EuroSAT*, which is split into 5 tasks. We distribute the data across 10 clients using the widely adopted *distribution-based* label imbalance setting [24, 53]. This approach partitions the data according to a Dirichlet distribution controlled by a β parameter. Additional results involving up to 100 clients are provided in the supplementary material.

For each dataset, we experiment with three different values of β , selected based on the number of examples. Specifically, we use $\beta \in \{0.5, 0.1, 0.05\}$ for *ImageNet-R* and *CIFAR-100*, and $\beta \in \{1.0, 0.5, 0.2\}$ for *EuroSAT*, *ImageNet-A*, *Cars-196* and *CUB-200*. This choice is imposed by the infeasibility of finding a valid split when either the data or the number of classes is limited. For all experiments, we evaluate the centralized model at the end of the training on the global test set.

Implementation Details. We use a pre-trained ViT-B/16 as the backbone for all compared methods, initializing the models with supervised pre-trained weights on ImageNet-21K [41]. For a comprehensive overview of the hyperparameters, please refer to the supplementary material. The results are averaged over three runs on different seeds. We report the standard deviations in the suppl. material.

Table 1: **Cifar-100, Imagenet-R and Imagenet-A.** Results in terms of FAA [\uparrow]. Best results are highlighted in bold, second-best underlined.

Joint	CIFAR-100			Imagenet-R			Imagenet-A		
	92.75			84.02			54.64		
Partition β	0.5	0.1	0.05	0.5	0.1	0.05	1.0	0.5	0.2
EWC	78.46	72.42	64.51	58.93	48.15	43.68	10.86	10.07	8.89
LwF	62.87	55.56	47.09	54.03	41.02	46.07	8.89	8.89	7.90
FisherAVG	76.10	74.43	65.31	58.68	50.82	47.33	11.59	11.06	10.14
RegMean	59.80	45.88	39.08	61.18	57.00	55.80	8.56	6.22	4.34
CCVR	79.95	75.14	65.30	70.00	62.60	60.38	39.50	36.27	35.94
L2P	83.88	61.54	55.00	42.08	23.85	16.98	20.14	17.31	16.85
DualPrompt	80.49	54.31	42.43	45.89	27.34	21.76	20.91	16.50	9.02
CODA-P	82.25	61.82	46.74	61.18	36.73	25.82	18.30	14.48	7.31
FedProto	75.79	70.02	60.55	58.52	47.30	52.93	9.87	9.22	10.01
TARGET	74.72	72.32	62.60	54.65	45.83	41.32	10.27	11.39	10.73
PIP	85.01	<u>81.87</u>	81.40	58.74	55.52	56.64	26.90	26.38	24.69
PILoRA	76.48	75.81	74.80	53.67	51.62	49.37	19.62	18.70	20.01
LoRM	<u>86.95</u>	81.75	<u>82.76</u>	<u>72.48</u>	<u>63.83</u>	<u>66.45</u>	37.26	<u>36.34</u>	33.11
HGP (ours)	90.39	90.20	90.16	72.64	71.93	71.58	41.61	41.01	40.62

4.2 Results

Metrics. We assess the performance of all methods using the widely adopted Final Average Accuracy (FAA). For the formal definition of such measure, we refer the reader to the suppl. material.

Evaluated approaches. Our proposal is evaluated alongside 13 competitors. Among these, *five* were originally designed for Class-Incremental Learning (CIL), *two* for Federated Learning (FL), *two* for Model Merging, and the remainder *four* for Federated Class-Incremental Learning (FCIL). Following common practice, we adapt CIL approaches for FCIL by aggregating local models with FedAvg [37]. From CIL, we include two regularization-based techniques (EWC [21], LwF [27]) and three prompting-based approaches (L2P [50], DualPrompt [49], and CODA-Prompt [44]). From FL, we select a rebalancing method (CCVR [31]), and one using a prototype-based classifier (FedProto [45]); we include two model merging techniques (FisherAVG [34] and RegMean [16]), and four FCIL methods. These leverage Parameter-Efficient Fine-Tuning (PILoRA [10]), generative replay (TARGET [56]), regularization prototypes (PIP [33]), and closed-form merging (LoRM [43]). Finally, we include the upper bound, where the same ViT-B/16 backbone is trained *jointly* on the global data distribution (*i.e.*, without federated or incremental splitting), referred to as "Joint".

Comparison. In Table 1, we present the results for CIFAR-100, Imagenet-R, and Imagenet-A. Consistently on the first two datasets, prompting methodologies struggle as the label heterogeneity in the data distribution increases. This aligns with our findings, suggesting that federated bias is more pronounced when learning prompts (see Section 4.3). In contrast, FisherAVG and LwF are steadier, but still exhibit poor performance overall. EWC and FisherAVG surprisingly perform similar to FL methodologies (CCVR, FedProto), only to be surpassed by FCIL-targeted approaches (PILoRA, PIP, TARGET, LoRM, HGP).

ImageNet-A, specifically designed to evaluate model robustness, poses a greater challenge by incorporating samples from ImageNet that are frequently misclassified. This is also evidenced by the lower performance of all methods. Here, classical CL techniques struggle to learn the task effectively and are surpassed by prompting methodologies. Among FL and FCIL approaches, only PIP and PILORA achieve decent performance, with CCVR and LoRM outperforming them. Finally, thanks to the combination of classifier rebalancing and prompting, HGP consistently delivers the best performance in all settings, while LoRM ranks as the second-best performer on average.

Table 2 compares the same methodologies on EuroSAT, Cars-196, and CUB-200. Among these datasets, Cars-196 is the most impacted by the FCIL setting, as it exhibits the largest performance gap

Table 2: **EuroSAT, Cars-196 and CUB-200**. Results in terms of FAA [\uparrow]. Best results are highlighted in bold, second-best underlined.

Joint	EuroSAT			Cars-196			CUB-200		
	98.42			85.62			86.04		
Partition β	0.5	0.1	0.05	0.5	0.1	0.05	1.0	0.5	0.2
EWC	64.12	59.30	56.52	19.55	18.02	18.29	31.46	29.60	27.89
LwF	31.91	21.26	31.42	20.84	22.72	31.76	25.25	21.11	18.54
FisherAVG	58.84	59.94	55.86	26.03	24.60	21.58	30.45	28.39	25.06
RegMean	48.74	51.73	45.27	21.83	20.36	15.92	35.57	32.84	32.83
CCVR	64.44	57.93	62.69	38.99	37.81	35.31	62.67	59.48	56.33
L2P	40.63	51.78	45.46	35.49	31.00	20.01	56.23	47.31	38.16
DualPrompt	62.97	52.78	55.34	34.07	26.47	21.30	60.93	55.59	44.61
CODA-P	73.38	69.42	66.69	28.04	20.83	14.53	42.53	37.71	29.19
FedProto	58.79	62.85	64.17	26.08	24.55	22.75	30.22	28.27	26.01
TARGET	52.74	52.74	45.11	28.65	27.20	26.13	39.30	38.40	34.79
PIP	58.12	53.67	54.16	36.02	34.33	29.99	69.60	65.46	60.79
PILoRA	48.35	32.89	31.22	37.57	37.92	36.95	61.11	60.68	60.39
LoRM	<u>84.23</u>	<u>77.26</u>	<u>81.36</u>	54.41	51.87	<u>48.81</u>	64.60	63.67	60.06
HGP (ours)	87.97	88.35	85.90	52.13	<u>51.48</u>	49.95	80.23	79.71	78.58

between joint training and the best-performing method. In this scenario, EWC and LwF fail to deliver satisfactory results, whereas FL and FCIL methodologies achieve competitive performance. While rebalancing played a critical role in the previously analyzed datasets, CCVR performs slightly worse than PILoRA in this case, highlighting the significant impact of low-rank adaptation. Here, HGP and LoRM compete for the top spot by a wide margin over the others, showing comparable performance.

For EuroSAT and CUB-200, the accuracy gap between Joint training and FCIL techniques narrows, suggesting a less challenging task. FedProto, CODA-Prompt, and DualPrompt demonstrate superior results on EuroSAT, whereas PIP, PILoRA and CCVR underperform on this dataset but achieve the best results on CUB-200. This trend reversal is likely due to the larger number of classes in CUB-200, which challenges traditional CL methods and highlights the significance of approaches specifically tailored for Federated Learning. LoRM emerges as the clear second-best performer on EuroSAT and struggles on CUB-200, where its performance aligns with that of PIP and PILoRA. HGP consistently delivers the highest performance across both datasets, with a notably large margin on CUB-200.

4.3 Ablation study

Impact of Different Components. We assess the specific contributions of various components of HGP in terms of FAA for three datasets under the most challenging distribution-based label imbalance setting ($\beta = 0.05$). Results of these ablative experiments are summarized in Table 3, where the full fine-tuning of ViT-B/16 serves as the lower bound. Incorporating our prompting technique yields a remarkable improvement on CIFAR-100 and Imagenet-R, with a minor gain on CUB-200. However, it is worth noting that the primary advantage of prompting lies not only in enhancing accuracy but also in confining bias to the final classification layer, thereby increasing the impact of Classifier Rebalancing.

We define CR_{cur} and CR_{old} as classifier rebalancing procedures applied to the current task classes and the old task classes, respectively. Specifically, CR_{cur} rebalances only the classification head for the current task by utilizing generated features from prototypes corresponding to the current classes. Conversely, CR_{old} focuses on rebalancing the classification heads for previous tasks by

Table 3: **HGP components**. Evaluation of the impact of each component of HGP. Presented in terms of FAA [\uparrow].

Prompt	CR_{old}	CR_{cur}	C-100	IN-R	CUB-200
\times	\times	\times	30.58	26.42	25.70
\checkmark	\times	\times	52.29	30.28	26.74
\checkmark	\checkmark	\times	81.91	66.70	69.51
\checkmark	\times	\checkmark	85.43	68.88	47.80
\checkmark	\checkmark	\checkmark	90.16	71.58	78.58

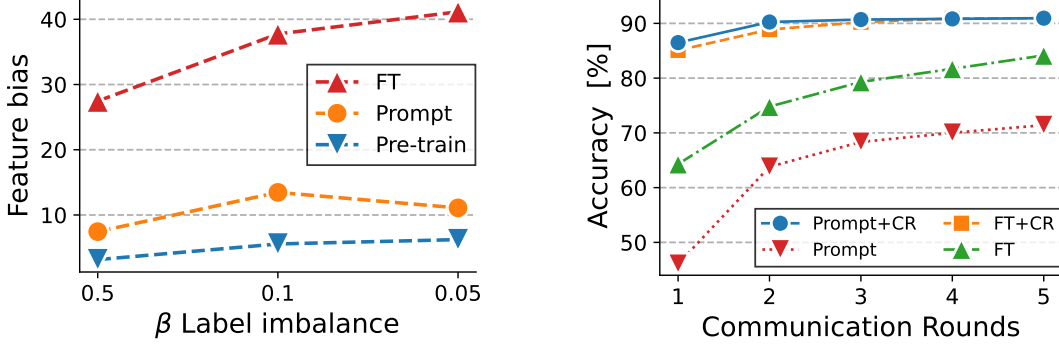


Figure 3: **Prompting vs. fine-tuning.** Average pairwise distance of the local prototypes on all clients (left). FL performance before and after Classifier Rebalancing (CR), for $\beta = 0.05$ (right).

sampling from the prototypes of the old classes. On average, both approaches perform comparably; however, CR_{old} demonstrates superior performance on CUB-200, highlighting the importance of addressing Incremental Bias in this dataset. By integrating all components, HGP demonstrates the critical contribution of each, achieving state-of-the-art performance as shown in Tables 1 and 2.

Prompting vs. fine-tuning. In this section, we explore the impact of prompting on Federated Bias, emphasizing the contrast with the traditional approach of fine-tuning the whole network. All experiments are performed on the CIFAR-100 dataset distributed across 10 clients.

We argue that prompting is a more advantageous approach for adapting pre-trained models in Federated Learning, as it constrains the bias to the last layer instead of distributing it across the whole network. To experimentally prove this claim, we position ourselves at the end of the local training prior to the first synchronization with the server: namely, when each client is trained exclusively on its local distribution. In this scenario, we assess the Federated Bias within the feature space – which we refer to as *feature bias* for short – by computing the local prototypes for the 10 clients and measuring their average *pairwise Euclidean distance*. Figure 3 (left) shows that prompting produces smaller feature bias compared to traditional fine-tuning, suggesting that the obtained features are less biased towards the local clients’ distributions. To validate this assertion, we also compute the same metric on the pre-trained model (ViT-B/16, on ImageNet-21k), which yields the smallest bias by design. This further supports our reasoning, as this last network experiences no fine-tuning whatsoever.

On the right-hand side of Figure 3, we show the performance of prompting *vs.* traditional fine-tuning. In line with recent works [55, 39, 36], prompting (Prompt) shows inferior performance compared to fine-tuning (FT), due to its limited plasticity. However, when leveraging Classifier Rebalancing (CR), we observe a reversal in this trend. Simply addressing Federated Bias in the last layer is sufficient for prompting to outperform classical fine-tuning: this suggests that prompting techniques train more biased classifiers while producing less biased features, effectively restricting FB to the final layer.

5 Relation with prior works

Federated Learning. In its most naive form, Federated Learning combines local models at the conclusion of each round through element-wise parameters averaging [37]. Other approaches introduce regularization techniques during local models’ training to prevent them from drifting too far from the centralized parameter space of the server. For instance, FedProx [25] and SCAFFOLD [17] explicitly enforce such regularization. FedDC [9] estimates the local parameter shift and employs it as a correction term before aggregating parameters. GradMA [30] addresses optimization challenges (*i.e.*, quadratic programming) by rerouting each client update towards optimizing the local problem while maintaining proximity to the server. On a different trajectory, the authors of [31] fit a Gaussian distribution for each class and use them to generate an IID dataset of features to calibrate the server’s classification head. FedProto [45] also computes prototypes for each class observed by each client but aggregates them into global prototypes; these serve as target representations for subsequent rounds. In contrast, our approach samples from a hierarchical Gaussian Mixture Model, and incorporates prompting to effectively isolate Federated Bias and Incremental Bias to the last layer.

Class-Incremental Learning. Class-Incremental Learning (CIL) stands out as one of the most challenging settings within the Continual Learning domain [46]. In this scenario, the training process is divided into tasks, each introducing new classes as the training progresses. To tackle this setting, early techniques rely on regularization, establishing checkpoints for previous tasks to maintain proximity w.r.t. their parameters [54, 21] or predictions [27]. Alternatively, rehearsal-based approaches involve storing samples in a limited memory buffer and subsequently replaying them to optimize either the original objective [42, 3] or a surrogate one based on knowledge distillation [40, 2].

Lately, the emergence of pre-trained self-attentive architectures [8] in the Computer Vision domain has paved the way for significant advancements, particularly with the advent of Parameter-Efficient Fine-Tuning (PEFT) techniques. Recent approaches [50, 49, 44] have harnessed prompting to achieve state-of-the-art performance in CIL, eliminating the need for a buffer to replay old samples. Instead, they employ a prompt pool comprising incrementally learned prompts, utilized to condition the network during the forward pass. In our approach, we adopt the prompting paradigm and introduce an efficient methodology that minimizes the computational overhead by eliminating the need for a double forward pass, ensuring state-of-the-art performance at the same time.

Federated Class-Incremental Learning. The concept of Federated Class-Incremental Learning (FCIL) was initially introduced in [52]. In their work, the authors propose FedWeIT, which partitions client-side parameters into task-generic and task-specific components. To mitigate interference between clients, they implement sparse learnable masks to selectively extract relevant knowledge for each client. GLFC [7] takes a different approach by combining local buffers with class-aware gradient compensation loss. This strategy helps counteract catastrophic forgetting through rehearsal, while also adjusting the magnitude of gradient updates based on whether input samples belong to new or old classes. Building upon this framework, an enhanced version is introduced by the same authors in the LGA paper [6]. TARGET [56] tackles forgetting by training a centralized generator network to produce synthetic data, maintaining a similar behavior to the generator used in previous tasks. The generative network populates a buffer after each task, allowing clients to utilize it for rehearsal. Recent advancements in FCIL involve fine-tuning pre-trained models using PEFT techniques. Fed-CPrompt [1] introduces a regularization term that encourages local prompts to diverge from global ones, enabling them to learn task-specific features. Instead, PILORA [10] integrates LoRA [14] with prototypes, which are aggregated via a re-weighting mechanism on the server side during each communication round, whereas LoRM [43] proposes a closed-form solution for merging parameter-efficient clients at the server side.

6 Conclusions

In this work, we propose Hierarchical Generative Prototypes (HGP), an approach aimed at mitigating Incremental and Federated Biases within Federated Class-Incremental Learning. HGP utilizes pre-trained architectures conditioned by prompting to achieve state-of-the-art performance while maintaining parameter efficiency. To tackle the problem of Federated Bias and Incremental Bias, we examine the implications of fine-tuning the entire model compared to using prompting techniques, demonstrating that the latter confines bias to the classification layer. Building on these insights, we propose Classifier Rebalancing – *i.e.*, sampling features from a hierarchical Gaussian Mixture Model to train the classifier across all observed classes – as an effective solution. Through the integration of prompt learning and Classifier Rebalancing, we achieve SOTA performance while learning only a minimal number of parameters.

Limitations and Future Works. This work builds upon Prompt Learning, which allows adapting a pre-trained architecture on a downstream task. Although leveraging a pre-trained model is a common strategy in Federated Learning literature [10, 29, 1], our findings may not extend to scenarios where models are trained from scratch. Moreover, although prompt tuning effectively localizes bias to the classifier layer, the behavior of other PEFT techniques – such as LoRA or Adapters – under continual decentralized scenarios remains unexplored. Investigating these methods may uncover important trade-offs between efficiency and bias control, which we leave for future work. Finally, assessing HGP’s robustness to adversarial settings with malicious clients remains an important direction, as it is critical for ensuring reliable deployment in real-world applications.

References

- [1] Gaurav Bagwe, Xiaoyong Yuan, Miao Pan, and Lan Zhang. Fed-cprompt: Contrastive prompt for rehearsal-free federated continual learning. In *Federated Learning and Analytics in Practice: Algorithms, Systems, Applications, and Opportunities*, 2023.
- [2] Pietro Buzzega, Matteo Boschini, Angelo Porrello, Davide Abati, and Simone Calderara. Dark experience for general continual learning: a strong, simple baseline. *Advances in Neural Information Processing Systems*, 2020.
- [3] Arslan Chaudhry, Marc’Aurelio Ranzato, Marcus Rohrbach, and Mohamed Elhoseiny. Efficient lifelong learning with a-gem. In *ICLR*, 2018.
- [4] Liam Collins, Hamed Hassani, Aryan Mokhtari, and Sanjay Shakkottai. Exploiting shared representations for personalized federated learning. In *International Conference on Machine Learning*, 2021.
- [5] Enmao Diao, Jie Ding, and Vahid Tarokh. Heterofl: Computation and communication efficient federated learning for heterogeneous clients. In *ICLR*, 2021.
- [6] Jiahua Dong, Hongliu Li, Yang Cong, Gan Sun, Yulun Zhang, and Luc Van Gool. No one left behind: Real-world federated class-incremental learning. *IEEE Transactions on Pattern Analysis and Machine Intelligence*, 2023.
- [7] Jiahua Dong, Lixu Wang, Zhen Fang, Gan Sun, Shichao Xu, Xiao Wang, and Qi Zhu. Federated class-incremental learning. In *CVPR*, 2022.
- [8] Alexey Dosovitskiy, Lucas Beyer, Alexander Kolesnikov, Dirk Weissenborn, Xiaohua Zhai, Thomas Unterthiner, Mostafa Dehghani, Matthias Minderer, Georg Heigold, Sylvain Gelly, et al. An image is worth 16x16 words: Transformers for image recognition at scale. In *ICLR*, 2020.
- [9] Liang Gao, Huazhu Fu, Li Li, Yingwen Chen, Ming Xu, and Cheng-Zhong Xu. Feddc: Federated learning with non-iid data via local drift decoupling and correction. In *CVPR*, 2022.
- [10] Haiyang Guo, Fei Zhu, Wenzhuo Liu, Xu-Yao Zhang, and Cheng-Lin Liu. Pilora: Prototype guided incremental lora for federated class-incremental learning. In *European Conference on Computer Vision*, pages 141–159. Springer, 2025.
- [11] Patrick Helber, Benjamin Bischke, Andreas Dengel, and Damian Borth. Introducing eurosat: A novel dataset and deep learning benchmark for land use and land cover classification. In *IEEE International Geoscience and Remote Sensing Symposium*, 2018.
- [12] Dan Hendrycks, Steven Basart, Norman Mu, Saurav Kadavath, Frank Wang, Evan Dorundo, Rahul Desai, Tyler Zhu, Samyak Parajuli, Mike Guo, et al. The many faces of robustness: A critical analysis of out-of-distribution generalization. In *ICCV*, 2021.
- [13] Dan Hendrycks, Kevin Zhao, Steven Basart, Jacob Steinhardt, and Dawn Song. Natural adversarial examples. In *Proceedings of the IEEE/CVF conference on computer vision and pattern recognition*, pages 15262–15271, 2021.
- [14] Edward J Hu, Phillip Wallis, Zeyuan Allen-Zhu, Yuanzhi Li, Shean Wang, Lu Wang, Weizhu Chen, et al. Lora: Low-rank adaptation of large language models. In *ICLR*, 2021.
- [15] Fatih Ilhan, Gong Su, and Ling Liu. Scalefl: Resource-adaptive federated learning with heterogeneous clients. In *CVPR*, 2023.
- [16] Xisen Jin, Xiang Ren, Daniel Preotiuc-Pietro, and Pengxiang Cheng. Dataless knowledge fusion by merging weights of language models. In *ICLR*, 2023.
- [17] Sai Praneeth Karimireddy, Satyen Kale, Mehryar Mohri, Sashank Reddi, Sebastian Stich, and Ananda Theertha Suresh. Scaffold: Stochastic controlled averaging for federated learning. In *International Conference on Machine Learning*, 2020.
- [18] Gyuhak Kim, Changnan Xiao, Tatsuya Konishi, Zixuan Ke, and Bing Liu. A theoretical study on solving continual learning. *Advances in Neural Information Processing Systems*, 2022.

[19] Minjae Kim, Sangyoon Yu, Suhyun Kim, and Soo-Mook Moon. Depthfl: Depthwise federated learning for heterogeneous clients. In *ICLR*, 2022.

[20] Diederik Kingma and Jimmy Ba. Adam: A method for stochastic optimization. In *ICLR*, 2015.

[21] James Kirkpatrick, Razvan Pascanu, Neil Rabinowitz, Joel Veness, Guillaume Desjardins, Andrei A Rusu, Kieran Milan, John Quan, Tiago Ramalho, Agnieszka Grabska-Barwinska, et al. Overcoming catastrophic forgetting in neural networks. *Proceedings of the National Academy of Sciences*, 2017.

[22] Jonathan Krause, Michael Stark, Jia Deng, and Li Fei-Fei. 3d object representations for fine-grained categorization. In *Proceedings of the IEEE International Conference on Computer Vision (ICCV) Workshops*, 2013.

[23] Alex Krizhevsky, Geoffrey Hinton, et al. Learning multiple layers of features from tiny images. *Master’s thesis, Department of Computer Science, University of Toronto*, 2009.

[24] Qinbin Li, Yiqun Diao, Quan Chen, and Bingsheng He. Federated learning on non-iid data silos: An experimental study. In *IEEE International Conference on Data Engineering*, 2022.

[25] Tian Li, Anit Kumar Sahu, Manzil Zaheer, Maziar Sanjabi, Ameet Talwalkar, and Virginia Smith. Federated optimization in heterogeneous networks. *Proceedings of Machine Learning and Systems*, 2020.

[26] Xiang Lisa Li and Percy Liang. Prefix-tuning: Optimizing continuous prompts for generation. In *Proceedings of the International Joint Conference on Natural Language Processing*, 2021.

[27] Zhizhong Li and Derek Hoiem. Learning without forgetting. *IEEE Transactions on Pattern Analysis and Machine Intelligence*, 2017.

[28] Jianhua Lin. Divergence measures based on the shannon entropy. *IEEE Transactions on information theory*, 1991.

[29] Chenghao Liu, Xiaoyang Qu, Jianzong Wang, and Jing Xiao. Fedet: a communication-efficient federated class-incremental learning framework based on enhanced transformer. In *IJCAI*, 2023.

[30] Kangyang Luo, Xiang Li, Yunshi Lan, and Ming Gao. Gradma: A gradient-memory-based accelerated federated learning with alleviated catastrophic forgetting. In *CVPR*, 2023.

[31] Mi Luo, Fei Chen, Dapeng Hu, Yifan Zhang, Jian Liang, and Jiashi Feng. No fear of heterogeneity: Classifier calibration for federated learning with non-iid data. *Advances in Neural Information Processing Systems*, 2021.

[32] Xiaosong Ma, Jie Zhang, Song Guo, and Wenchao Xu. Layer-wised model aggregation for personalized federated learning. In *CVPR*, 2022.

[33] Muhammad Anwar Ma’sum, Mahardhika Pratama, Savitha Ramasamy, Lin Liu, Habibullah Habibullah, and Ryszard Kowalczyk. Pip: Prototypes-injected prompt for federated class incremental learning. In *Proceedings of the 33rd ACM International Conference on Information and Knowledge Management*, pages 1670–1679, 2024.

[34] Michael S Matena and Colin A Raffel. Merging models with fisher-weighted averaging. *Advances in Neural Information Processing Systems*, 2022.

[35] Michael McCloskey and Neal J Cohen. Catastrophic interference in connectionist networks: The sequential learning problem. In *Psychology of learning and motivation*, 1989.

[36] Mark D McDonnell, Dong Gong, Amin Parvaneh, Ehsan Abbasnejad, and Anton van den Hengel. Ranpac: Random projections and pre-trained models for continual learning. *Advances in Neural Information Processing Systems*, 2024.

[37] Brendan McMahan, Eider Moore, Daniel Ramage, Seth Hampson, and Blaise Aguera y Arcas. Communication-efficient learning of deep networks from decentralized data. In *International Conference on Artificial Intelligence and Statistics*, 2017.

[38] JAE HOON OH, Sangmook Kim, and Seyoung Yun. Fedbabu: Toward enhanced representation for federated image classification. In *ICLR*, 2022.

[39] Aristeidis Panos, Yuriko Kobe, Daniel Olmeda Reino, Rahaf Aljundi, and Richard E Turner. First session adaptation: A strong replay-free baseline for class-incremental learning. In *ICCV*, 2023.

[40] Sylvestre-Alvise Rebuffi, Alexander Kolesnikov, Georg Sperl, and Christoph H Lampert. icarl: Incremental classifier and representation learning. In *CVPR*, 2017.

[41] Tal Ridnik, Emanuel Ben-Baruch, Asaf Noy, and Lihi Zelnik-Manor. Imagenet-21k pretraining for the masses. In *Conference on Neural Information Processing Systems Datasets and Benchmarks Track (Round 1)*, 2021.

[42] Anthony Robins. Catastrophic forgetting, rehearsal and pseudorehearsal. *Connection Science*, 1995.

[43] Riccardo Salami, Pietro Buzzega, Matteo Mosconi, Jacopo Bonato, Luigi Sabetta, and Simone Calderara. Closed-form merging of parameter-efficient modules for federated continual learning. *ICLR*, 2025.

[44] James Seale Smith, Leonid Karlinsky, Vyshnavi Gutta, Paola Cascante-Bonilla, Donghyun Kim, Assaf Arbelle, Rameswar Panda, Rogerio Feris, and Zsolt Kira. Coda-prompt: Continual decomposed attention-based prompting for rehearsal-free continual learning. In *CVPR*, 2023.

[45] Yue Tan, Guodong Long, Lu Liu, Tianyi Zhou, Qinghua Lu, Jing Jiang, and Chengqi Zhang. Fedproto: Federated prototype learning across heterogeneous clients. In *AAAI*, 2022.

[46] Gido M. van de Ven, Tinne Tuytelaars, and Andreas Savas Tolias. Three types of incremental learning. *Nature Machine Intelligence*, 2022.

[47] C. Wah, S. Branson, P. Welinder, P. Perona, and S. Belongie. Caltech-ucsd birds-200-2011. Technical Report CNS-TR-2011-001, California Institute of Technology, 2011.

[48] Alastair J Walker. New fast method for generating discrete random numbers with arbitrary frequency distributions. *Electronics Letters*, 1974.

[49] Zifeng Wang, Zizhao Zhang, Sayna Ebrahimi, Ruoxi Sun, Han Zhang, Chen-Yu Lee, Xiaoqi Ren, Guolong Su, Vincent Perot, Jennifer Dy, et al. Dualprompt: Complementary prompting for rehearsal-free continual learning. In *ECCV*, 2022.

[50] Zifeng Wang, Zizhao Zhang, Chen-Yu Lee, Han Zhang, Ruoxi Sun, Xiaoqi Ren, Guolong Su, Vincent Perot, Jennifer Dy, and Tomas Pfister. Learning to prompt for continual learning. In *CVPR*, 2022.

[51] Yue Wu, Yinpeng Chen, Lijuan Wang, Yuancheng Ye, Zicheng Liu, Yandong Guo, and Yun Fu. Large scale incremental learning. In *CVPR*, 2019.

[52] Jaehong Yoon, Wonyong Jeong, Giwoong Lee, Eunho Yang, and Sung Ju Hwang. Federated continual learning with weighted inter-client transfer. In *International Conference on Machine Learning*, 2021.

[53] Mikhail Yurochkin, Mayank Agarwal, Soumya Ghosh, Kristjan Greenewald, Nghia Hoang, and Yasaman Khazaeni. Bayesian nonparametric federated learning of neural networks. In *International Conference on Machine Learning*, 2019.

[54] Friedemann Zenke, Ben Poole, and Surya Ganguli. Continual learning through synaptic intelligence. In *International Conference on Machine Learning*, 2017.

[55] Gengwei Zhang, Liyuan Wang, Guoliang Kang, Ling Chen, and Yunchao Wei. Slca: Slow learner with classifier alignment for continual learning on a pre-trained model. In *ICCV*, 2023.

[56] Jie Zhang, Chen Chen, Weiming Zhuang, and Lingjuan Lyu. Target: Federated class-continual learning via exemplar-free distillation. In *ICCV*, 2023.

- [57] Haodong Zhao, Wei Du, Fangqi Li, Peixuan Li, and Gongshen Liu. Fedprompt: Communication-efficient and privacy-preserving prompt tuning in federated learning. In *ICASSP*, 2023.
- [58] Nanxuan Zhao, Zhirong Wu, Rynson WH Lau, and Stephen Lin. What makes instance discrimination good for transfer learning? In *ICLR*, 2020.
- [59] Yue Zhao, Meng Li, Liangzhen Lai, Naveen Suda, Damon Civin, and Vikas Chandra. Federated learning with non-iid data. *arXiv preprint arXiv:1806.00582*, 2018.

A Communication Cost

Efficient communication is paramount in Federated Learning because of the extensive coordination required between server and clients. In this section, we analyze illustrates the relationship between Final Average Accuracy (FAA) and communication cost for each method. The FAA results are provided for CUB-200 (Figure B), Imagenet-R, and CIFAR-100 (Figure A), with $\beta = 0.05$, and communication costs are measured in Megabytes (MB) per communication round, representing the average data exchanged between a single client and the server.

Notably, methods that do not utilize PEFT techniques incur significantly higher communication costs, as they optimize all parameters. Consequently, with larger models, communication costs escalate proportionally without corresponding performance gains. TARGET is the most expensive method overall because the server sends the entire model and the generated dataset to clients once per task. In contrast, the adoption of PEFT techniques enhances both efficiency and performance. L2P emerges as the most efficient method, using fewer prompts than its competitors, followed by DualPrompt and CODA-P. PILoRA is on par to the previous prompt-based solutions in terms of efficiency. HGP demonstrates efficiency comparable with the PEFT techniques, ensuring a strong performance gain.

Overall, the efficiency gains and substantial performance improvements offered by PEFT techniques highlight their advantage in Federated Learning scenarios.

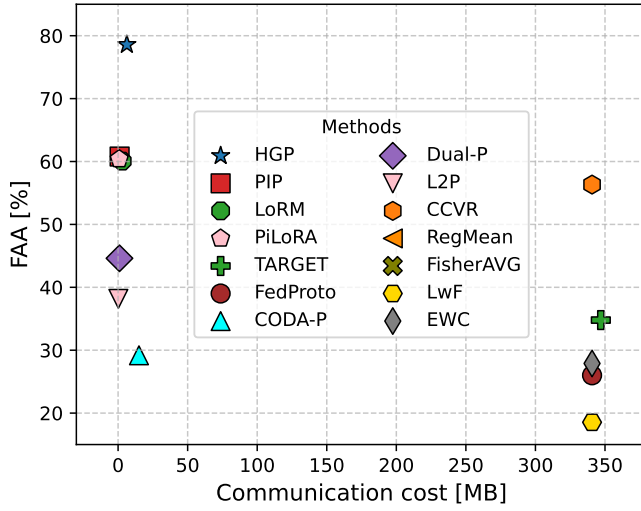


Figure B: FAA [%] in relation with the communication cost [MB] for all tested approaches on CUB-200.

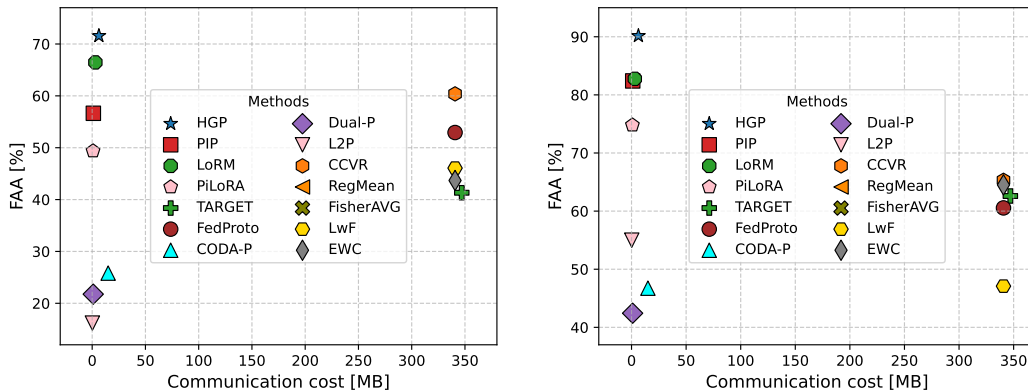


Figure A: FAA [%] in relation with the communication cost [MB] for all tested approaches on Imagenet-R (left) and CIFAR-100 (right).

B Computational Complexity

Our experimental setup aligns with prior work, assuming clients can fine-tune transformer-based networks. However, our method reduces training cost significantly by using prompt tuning, updating only $\sim 1.5\%$ of the total model parameters.

To ensure efficiency and numerical stability, we employ diagonal covariance matrices (represented as vectors) as prototypes. Empirically, full covariance matrices provide no accuracy gains and incur higher computation and memory costs.

Constructing and updating the hierarchical mixture model incurs negligible cost, as it only requires maintaining running statistics. Sampling from the mixture involves two categorical draws (for client and class selection) and one Gaussian draw (for synthetic features). Thanks to the Alias method [48], categorical sampling is performed in $\mathcal{O}(1)$, and Gaussian sampling in $\mathcal{O}(\text{features_dim})$.

In total, the sampling cost is approximately 770 FLOPs for ViT-B/16. For comparison, a single forward pass on ViT-B/16 requires ~ 17 GFLOPs, making our sampling overhead negligible. Moreover, inference time is further reduced by our proposed prompting technique, which employs a single shared prompt rather than a prompt pool thus decreasing inference cost by up to 50%.

C Implementation Details

C.1 Hyperparameters

We utilize a pre-trained ViT-B/16 as the backbone for HGP and all the compared methods. Specifically, we initialize the models with supervised pre-trained weights on ImageNet-21K [41] for all datasets.

In our method, we adopt a single prompt for all tasks, negating both the need for a double forward pass while also avoiding the need to store old task-specific parameters. Across all experiments, prompt components have a shape of $(200, d)$, where $d = 768$ represents the embedding dimension for the chosen architecture. We train said prompt using prefix tuning, conditioning the first 5 layers of the backbone. For each task, we perform five communication rounds, during which clients observe their local datasets for five epochs with a batch size of 16. Training is conducted using the Adam optimizer [20] with a learning rate of 0.003; β_1 and β_2 are set to 0.9 and 0.999, respectively.

The centralized server rebalances the global classifier for five epochs. We use the SGD optimizer with a learning rate of 0.01 and a momentum of 0.9, with a batch size of 256, and also apply a cosine annealing learning rate scheduler. We generate an average of 256 feature vectors for each class encountered up to this point, multiplying the covariance associated with each prototype by 3 to enhance dataset diversity. All images are resized to 224×224 using bicubic interpolation and scaled to ensure their values fall within the range $[0, 1]$. Additionally, we employ random cropping and horizontal flipping as data augmentation techniques. All experiments are conducted on a single Nvidia RTX5000 GPU.

The specific training details for all implemented methods are documented in Appendix H.

C.2 Metrics

We assess the performance of all methods using the most commonly used metric in FCIL literature: Final Average Accuracy (FAA).

FAA represents the mean accuracy on all observed tasks at the conclusion of the incremental training process. Mathematically, if A_i^j denotes the accuracy on the i^{th} task at the j^{th} incremental step, where $i \leq j$, FAA can be expressed as:

$$\text{FAA} = \frac{1}{T} \sum_{i=1}^T A_i^T.$$

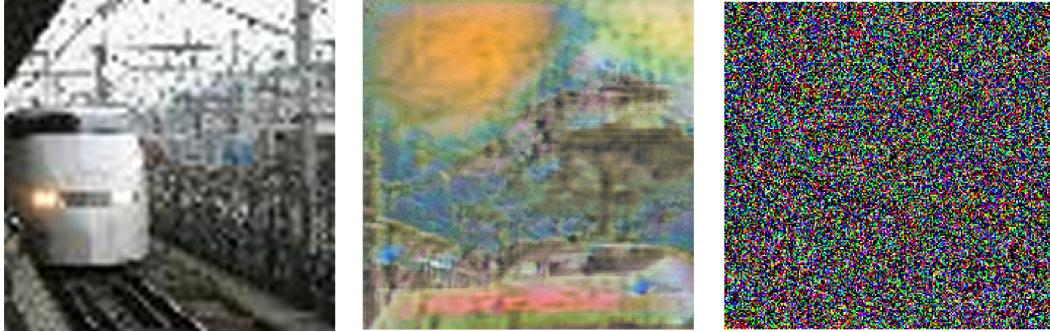


Figure C: Real training image (left) and its reconstructions leveraging either the input image (center) or the generative prototype of the related class (right).

D Prototypes of Features are Privacy-preserving

In Federated Learning, maintaining the privacy of local data distributions is of utmost importance. It is crucial that no private samples are directly transmitted from the client to the server. In the HGP framework, each client provide the server with a generative prototype for each observed class.

To verify the safety of generative prototypes, we firstly examine a hypothetical scenario where an attacker gains access to the trained model along with a real image utilized during training. In such a case, the attacker could potentially employ the feature inversion technique outlined in [58]. This methodology provides for training a autoencoder to precisely match the input image. Specifically, the autoencoder takes fixed noise as input and reconstructs the image. Then, both the real and reconstructed image are passed through the frozen backbone. The objective is to minimize the mean squared error (MSE) loss between their respective features. Figure C (left) shows the real training image from the Tiny-ImageNet dataset, while Figure C (center) displays the reconstruction obtained by the trained autoencoder. Through this process, no significant semantics can be recovered. At most, the class might be guessed, but the image does not provide any detail of the original sample.

In another setting, we suppose that the attacker gains access to the centralized server, which has visibility into clients' generative prototypes. To recover an input image, initial random noise in the input space is optimized by minimizing MSE between its features and those of a fixed sample from the generative prototype. Figure C (right) shows that this results in a shapeless, noisy reconstruction, making it impracticable for an attacker to recreate real images from these feature distributions.

E Scalability to Large Client Populations

To assess the scalability of our approach, we conducted additional experiments on CIFAR-100 using 100 clients with varying participation rates under extreme distribution imbalance ($\beta = 0.05$). Specifically, we tested participation rates of 10%, 20%, 50%, and 100%, obtaining average accuracies of 80.82%, 87.33%, 89.51%, and 90.08%, respectively. These results demonstrate that our method remains robust even under the most challenging federated settings, with only 10 clients participating per round. Remarkably, in this low-participation regime, our method still outperforms all competing methods evaluated with just 10 clients and full participation.

F Algorithm

Algorithm 1 provides the pseudo-code for a generic task t in the HGP framework.

Algorithm 1 Hierarchical Generative Prototypes HGP

```

1: Input: generic task  $t$ ;  $M$  clients; local model  $f_{\theta_m^t}(\cdot)$  parameterized by  $\theta_m^t = \{\mathcal{P}_m, W_m^t\}$ ;  $N$  prompts;  $C$  classes;  $E$  local epochs;  $E_r$  rebalancing epochs; local learning rate  $\eta$ ; rebalancing learning rate  $\eta_r$ .
2: for each communication round do
3:   Server side:
4:     Server distributes  $\theta^t$ 
5:   Client side:
6:     for each client  $m \in \{1, \dots, M\}$  in parallel do
7:        $\theta_m^t = \theta^t$ 
8:       for each local epoch  $e \in \{1, \dots, E\}$  do
9:         for each batch  $(x, y) \sim D_m^t$  do
10:           $\theta_m^t \leftarrow \theta_m^t - \eta \nabla \mathcal{L}_{\text{CE}}(f_{\theta_m^t}(x), y)$ 
11:        end for
12:      end for
13:      Compute feature vectors  $h$  on  $D_m^t$ 
14:      for each class  $c \in C^t$  do
15:        Compute  $\mu_{m,c}$  and  $\Sigma_{m,c}$  to parameterize  $\mathcal{N}_{m,c}$ 
16:      end for
17:      Send parameters  $\theta_m^t$  and Gaussians  $\mathcal{N}_{m,c}$  to the server
18:    end for
19:    Server side:
20:    Compute  $\theta^t = \frac{1}{|D^t|} \sum_{m=1}^M |D_m^t| \theta_m^t$ 
21:    for each class  $c \in C^t$  do
22:      Compute  $\tilde{Q}_c = \sum_{m=1}^M \pi_{m,c} \mathcal{N}_{m,c}(\mu_{m,c}, \Sigma_{m,c})$ 
23:    end for
24:    Compute  $\tilde{Q} = \sum_{c=1}^C \omega_c \tilde{Q}_c$ 
25:    Collect dataset  $\hat{D}$  by sampling feature vectors from  $\tilde{Q}$ 
26:    for each rebalancing epoch  $e \in \{1, \dots, E_r\}$  do
27:      Optimize  $W$  using equation 7 (main paper)
28:    end for
29:  end for

```

G Standard Deviations

The standard deviations across three runs for each method are presented in Table A and Table B.

Table A: Standard deviations (reported in FAA) for CIFAR-100, ImageNet-R and ImageNet-A.

Distrib. β	CIFAR-100			ImageNet-R			ImageNet-A		
	0.5	0.1	0.05	0.5	0.1	0.05	1.0	0.5	0.2
EWC	1.38	2.32	2.67	1.69	1.14	1.14	1.34	0.75	1.38
LwF	1.15	2.38	4.25	1.91	0.93	1.38	0.30	0.27	1.61
FisherAVG	0.40	3.67	3.18	0.77	0.47	0.93	1.59	1.36	1.49
RegMean	0.01	1.78	4.87	1.10	0.85	1.44	0.59	1.10	0.70
CCVR	1.13	2.49	1.39	0.57	0.49	2.29	1.19	0.63	2.26
L2P	1.62	1.49	1.85	1.17	1.61	1.35	0.72	0.81	2.01
DualPrompt	2.17	3.33	1.42	0.83	1.68	1.35	0.34	1.70	0.86
CODA-P	1.15	1.96	0.96	0.98	1.95	1.19	0.16	1.63	0.22
FedProto	2.05	0.94	1.96	2.09	2.28	0.72	1.18	0.71	2.17
TARGET	0.79	1.02	1.81	0.33	1.58	1.21	0.65	0.46	1.34
PILoRA	0.28	0.98	4.08	0.29	1.01	0.33	0.08	0.31	0.33
PIP	0.29	1.32	0.68	0.52	0.48	0.34	0.78	0.20	0.83
LoRM	0.27	0.20	0.79	0.04	0.16	0.87	0.86	0.75	0.68
HGP	0.08	0.14	0.24	0.43	0.39	0.31	0.90	0.91	0.29

Table B: Standard deviations (reported in FAA) for EuroSAT, Cars-196, and CUB-200.

Distrib. β	EuroSAT			Cars-196			CUB-200		
	1.0	0.5	0.2	1.0	0.5	0.2	1.0	0.5	0.2
EWC	7.33	5.78	6.60	1.72	0.46	1.00	0.55	0.94	1.68
LwF	3.32	4.58	5.12	1.35	2.81	2.01	2.07	2.15	2.02
FisherAVG	5.43	6.07	3.40	2.10	1.78	0.78	0.26	1.35	2.21
RegMean	3.99	7.21	5.68	0.23	1.11	1.80	1.79	2.63	2.27
CCVR	9.01	7.16	6.26	1.49	0.87	2.08	1.22	1.69	1.73
L2P	2.52	3.49	2.02	0.87	1.94	0.36	2.38	0.78	1.21
DualPrompt	8.75	6.70	8.89	0.87	1.79	1.82	0.42	2.62	2.69
CODA-P	4.52	6.27	6.54	1.05	2.24	1.89	0.51	1.52	1.86
FedProto	3.58	8.74	7.96	1.11	0.35	0.87	0.96	0.67	1.99
TARGET	4.12	6.20	5.31	0.93	0.68	1.54	1.17	0.65	2.06
PILoRA	4.45	4.07	4.27	0.21	0.33	0.18	0.51	0.28	0.51
PIP	5.95	0.49	2.61	1.11	2.15	4.01	1.90	1.10	1.42
LoRM	1.75	3.34	6.51	1.07	0.26	0.92	0.86	0.98	0.44
HGP	1.03	1.20	1.37	1.73	1.58	0.30	0.36	0.19	0.60

H Hyperparameter Tables

The following acronyms and symbols are used throughout the paper: lr denotes the learning rate; lr_{pr} refers to the learning rate applied to prototypes; λ_{KL} is the weighting factor for the Knowledge Distillation (KL) loss; r represents the rank used in low-rank matrix approximations; g_{ep} indicates the number of epochs used for training and sample generation in the generator network; and γ is the decay coefficient applied to the off-diagonal elements of the Gram matrices for the backbone (first component) and classifier (second component).

H.1 CIFAR-100

β	0.5	0.1	0.05
EwC	<i>lr</i> : 1e-5	<i>lr</i> : 1e-5	<i>lr</i> : 1e-5
LwF	<i>lr</i> : 1e-5	<i>lr</i> : 1e-5	<i>lr</i> : 1e-5
FisherAVG	<i>lr</i> : 1e-5	<i>lr</i> : 1e-5	<i>lr</i> : 1e-5
RegMean	<i>lr</i> : 1e-5; γ : (0.5, 0.5)	<i>lr</i> : 1e-5; γ : (0.5, 0.5)	<i>lr</i> : 1e-5; γ : (0.5, 0.5)
CCVR	<i>lr</i> : 1e-5	<i>lr</i> : 1e-5	<i>lr</i> : 1e-5
L2P	<i>lr</i> : 3e-2	<i>lr</i> : 3e-2	<i>lr</i> : 3e-2
DualPrompt	<i>lr</i> : 5e-2	<i>lr</i> : 5e-2	<i>lr</i> : 5e-2
CODA-P	<i>lr</i> : 1e-3	<i>lr</i> : 1e-3	<i>lr</i> : 1e-3
FedProto	<i>lr</i> : 1e-5	<i>lr</i> : 1e-5	<i>lr</i> : 1e-5
TARGET	<i>lr</i> : 1e-5; λ_{KL} : 25; g_{ep} : 30	<i>lr</i> : 1e-5; λ_{KL} : 25; g_{ep} : 30	<i>lr</i> : 1e-5; λ_{KL} : 25; g_{ep} : 30
PILoRA	<i>lr</i> : 2e-2; lr_{pr} : 1e-4	<i>lr</i> : 2e-2; lr_{pr} : 1e-4	<i>lr</i> : 2e-2; lr_{pr} : 1e-4
PIP	<i>lr</i> : 5e-3	<i>lr</i> : 5e-3	<i>lr</i> : 5e-3
LoRM	<i>lr</i> : 3e-4; r : 1 γ : (0, 0.5)	<i>lr</i> : 1e-4; r : 16 γ : (0, 0.5)	<i>lr</i> : 5e-4; r : 16 γ : (0, 0.5)
HGP	<i>lr</i> : 3e-3	<i>lr</i> : 3e-3	<i>lr</i> : 3e-3

H.2 ImageNet-R

β	0.5	0.1	0.05
EwC	<i>lr</i> : 1e-5	<i>lr</i> : 1e-5	<i>lr</i> : 1e-5
LwF	<i>lr</i> : 1e-5	<i>lr</i> : 1e-5	<i>lr</i> : 3e-5
FisherAVG	<i>lr</i> : 1e-5	<i>lr</i> : 1e-5	<i>lr</i> : 1e-5
RegMean	<i>lr</i> : 1e-5; γ : (0.1, 0.1)	<i>lr</i> : 1e-5; γ : (0.1, 0.1)	<i>lr</i> : 1e-5; γ : (0.1, 0.1)
CCVR	<i>lr</i> : 1e-5	<i>lr</i> : 1e-5	<i>lr</i> : 1e-5
L2P	<i>lr</i> : 3e-2	<i>lr</i> : 3e-2	<i>lr</i> : 3e-2
DualPrompt	<i>lr</i> : 3e-4	<i>lr</i> : 3e-4	<i>lr</i> : 3e-4
CODA-P	<i>lr</i> : 1e-3	<i>lr</i> : 1e-3	<i>lr</i> : 1e-3
FedProto	<i>lr</i> : 1e-5	<i>lr</i> : 1e-5	<i>lr</i> : 3e-5
TARGET	<i>lr</i> : 1e-5; λ_{KL} : 25; g_{ep} : 30	<i>lr</i> : 1e-5; λ_{KL} : 25; g_{ep} : 30	<i>lr</i> : 1e-5; λ_{KL} : 25; g_{ep} : 30
PILoRA	<i>lr</i> : 2e-2; lr_{pr} : 1e-4	<i>lr</i> : 2e-2; lr_{pr} : 1e-4	<i>lr</i> : 2e-2; lr_{pr} : 1e-4
PIP	<i>lr</i> : 3e-4	<i>lr</i> : 3e-4	<i>lr</i> : 3e-4
LoRM	<i>lr</i> : 3e-3; r : 2 γ : (0, 0.5)	<i>lr</i> : 1e-3; r : 32 γ : (0, 0.5)	<i>lr</i> : 1e-3; r : 16 γ : (0, 0.5)
HGP	<i>lr</i> : 3e-2	<i>lr</i> : 3e-2	<i>lr</i> : 1e-2

H.3 ImageNet-A

β	1.0	0.5	0.2
EwC	<i>lr</i> : 1e-5	<i>lr</i> : 1e-5	<i>lr</i> : 1e-5
LwF	<i>lr</i> : 1e-5	<i>lr</i> : 1e-5	<i>lr</i> : 3e-5
FisherAVG	<i>lr</i> : 1e-5	<i>lr</i> : 1e-5	<i>lr</i> : 1e-5
RegMean	<i>lr</i> : 1e-5; γ : (0.1, 0.1)	<i>lr</i> : 1e-5; γ : (0.1, 0.1)	<i>lr</i> : 1e-5; γ : (0.1, 0.1)
CCVR	<i>lr</i> : 1e-5	<i>lr</i> : 1e-5	<i>lr</i> : 1e-5
L2P	<i>lr</i> : 3e-2	<i>lr</i> : 3e-2	<i>lr</i> : 3e-1
DualPrompt	<i>lr</i> : 3e-2	<i>lr</i> : 3e-2	<i>lr</i> : 3e-2
CODA-P	<i>lr</i> : 1e-2	<i>lr</i> : 1e-2	<i>lr</i> : 1e-2
FedProto	<i>lr</i> : 3e-5	<i>lr</i> : 1e-5	<i>lr</i> : 1e-5
TARGET	<i>lr</i> : 1e-4; λ_{KL} : 25; g_{ep} : 30	<i>lr</i> : 1e-4; λ_{KL} : 25; g_{ep} : 30	<i>lr</i> : 1e-4; λ_{KL} : 25; g_{ep} : 30
PILoRA	<i>lr</i> : 2e-2; lr_{pr} : 1e-4	<i>lr</i> : 1e-2; lr_{pr} : 1e-4	<i>lr</i> : 2e-2; lr_{pr} : 1e-4
PIP	<i>lr</i> : 3e-2	<i>lr</i> : 3e-2	<i>lr</i> : 3e-2
LoRM	<i>lr</i> : 1e-2; r : 4 γ : (0, 0.5)	<i>lr</i> : 1e-2; r : 4 γ : (0, 0.5)	<i>lr</i> : 1e-2; r : 4 γ : (0, 0.5)
HGP	<i>lr</i> : 3e-2	<i>lr</i> : 3e-2	<i>lr</i> : 3e-2

H.4 EuroSAT

β	1.0	0.5	0.2
EwC	<i>lr</i> : 1e-5	<i>lr</i> : 1e-5	<i>lr</i> : 1e-5
LwF	<i>lr</i> : 1e-5	<i>lr</i> : 1e-5	<i>lr</i> : 3e-5
FisherAVG	<i>lr</i> : 1e-5	<i>lr</i> : 1e-5	<i>lr</i> : 1e-5
RegMean	<i>lr</i> : 1e-5; γ : (0.1, 0.1)	<i>lr</i> : 1e-5; γ : (0.1, 0.1)	<i>lr</i> : 1e-5; γ : (0.1, 0.1)
CCVR	<i>lr</i> : 1e-5	<i>lr</i> : 1e-5	<i>lr</i> : 1e-5
L2P	<i>lr</i> : 3e-2	<i>lr</i> : 3e-2	<i>lr</i> : 3e-2
DualPrompt	<i>lr</i> : 1e-3	<i>lr</i> : 1e-3	<i>lr</i> : 1e-3
CODA-P	<i>lr</i> : 1e-3	<i>lr</i> : 1e-3	<i>lr</i> : 1e-3
FedProto	<i>lr</i> : 3e-5	<i>lr</i> : 1e-5	<i>lr</i> : 1e-5
TARGET	<i>lr</i> : 1e-5; λ_{KL} : 25; g_{ep} : 30	<i>lr</i> : 1e-5; λ_{KL} : 25; g_{ep} : 30	<i>lr</i> : 1e-5; λ_{KL} : 25; g_{ep} : 30
PILoRA	<i>lr</i> : 2e-2; lr_{pr} : 1e-4	<i>lr</i> : 2e-2; lr_{pr} : 1e-4	<i>lr</i> : 2e-2; lr_{pr} : 1e-4
PIP	<i>lr</i> : 1e-3	<i>lr</i> : 1e-3	<i>lr</i> : 1e-3
LoRM	<i>lr</i> : 3e-3; r : 1 γ : (0, 0.5)	<i>lr</i> : 3e-3; r : 1 γ : (0, 0.5)	<i>lr</i> : 1e-3; r : 4 γ : (0, 0.5)
HGP	<i>lr</i> : 1e-3	<i>lr</i> : 3e-4	<i>lr</i> : 1e-4

H.5 Cars-196

β	1.0	0.5	0.2
EwC	<i>lr</i> : 1e-5	<i>lr</i> : 1e-5	<i>lr</i> : 1e-5
LwF	<i>lr</i> : 1e-5	<i>lr</i> : 1e-5	<i>lr</i> : 3e-5
FisherAVG	<i>lr</i> : 1e-5	<i>lr</i> : 1e-5	<i>lr</i> : 1e-5
RegMean	<i>lr</i> : 1e-5; γ : (0.1, 0.1)	<i>lr</i> : 1e-5; γ : (0.1, 0.1)	<i>lr</i> : 1e-5; γ : (0.1, 0.1)
CCVR	<i>lr</i> : 1e-5	<i>lr</i> : 1e-5	<i>lr</i> : 1e-5
L2P	<i>lr</i> : 3e-2	<i>lr</i> : 3e-2	<i>lr</i> : 3e-2
DualPrompt	<i>lr</i> : 1e-1	<i>lr</i> : 1e-1	<i>lr</i> : 1e-1
CODA-P	<i>lr</i> : 3e-2	<i>lr</i> : 3e-2	<i>lr</i> : 3e-2
FedProto	<i>lr</i> : 1e-5	<i>lr</i> : 1e-5	<i>lr</i> : 1e-5
TARGET	<i>lr</i> : 1e-4; λ_{KL} : 25; g_{ep} : 30	<i>lr</i> : 1e-4; λ_{KL} : 25; g_{ep} : 30	<i>lr</i> : 1e-4; λ_{KL} : 25; g_{ep} : 30
PILoRA	<i>lr</i> : 1e-1; lr_{pr} : 1e-4	<i>lr</i> : 1e-1; lr_{pr} : 1e-4	<i>lr</i> : 1e-1; lr_{pr} : 1e-4
PIP	<i>lr</i> : 1e-1	<i>lr</i> : 1e-1	<i>lr</i> : 1e-1
LoRM	<i>lr</i> : 1e-2; r : 8 γ : (0, 0.5)	<i>lr</i> : 1e-2; r : 8 γ : (0, 0.5)	<i>lr</i> : 1e-2; r : 4 γ : (0, 0.5)
HGP	<i>lr</i> : 3e-3	<i>lr</i> : 3e-3	<i>lr</i> : 3e-3

H.6 CUB-200

β	1.0	0.5	0.2
EwC	<i>lr</i> : 1e-5	<i>lr</i> : 1e-5	<i>lr</i> : 1e-5
LwF	<i>lr</i> : 1e-5	<i>lr</i> : 1e-5	<i>lr</i> : 3e-5
FisherAVG	<i>lr</i> : 1e-5	<i>lr</i> : 1e-5	<i>lr</i> : 1e-5
RegMean	<i>lr</i> : 1e-5; γ : (0.1, 0.1)	<i>lr</i> : 1e-5; γ : (0.1, 0.1)	<i>lr</i> : 1e-5; γ : (0.1, 0.1)
CCVR	<i>lr</i> : 1e-5	<i>lr</i> : 1e-5	<i>lr</i> : 1e-5
L2P	<i>lr</i> : 3e-1	<i>lr</i> : 3e-1	<i>lr</i> : 3e-1
DualPrompt	<i>lr</i> : 1e-1	<i>lr</i> : 1e-1	<i>lr</i> : 1e-1
CODA-P	<i>lr</i> : 1e-3	<i>lr</i> : 1e-3	<i>lr</i> : 1e-3
FedProto	<i>lr</i> : 1e-5	<i>lr</i> : 1e-5	<i>lr</i> : 1e-5
TARGET	<i>lr</i> : 1e-4; λ_{KL} : 25; g_{ep} : 30	<i>lr</i> : 1e-4; λ_{KL} : 25; g_{ep} : 30	<i>lr</i> : 1e-4; λ_{KL} : 25; g_{ep} : 30
PILoRA	<i>lr</i> : 1; lr_{pr} : 1e-4	<i>lr</i> : 1; lr_{pr} : 1e-4	<i>lr</i> : 1; lr_{pr} : 1e-4
PIP	<i>lr</i> : 1e-1	<i>lr</i> : 1e-1	<i>lr</i> : 1e-1
LoRM	<i>lr</i> : 1e-2; r : 1 γ : (0, 0.3)	<i>lr</i> : 3e-2; r : 1 γ : (0, 0.3)	<i>lr</i> : 3e-2; r : 1 γ : (0, 0.3)
HGP	<i>lr</i> : 1e-1	<i>lr</i> : 1e-1	<i>lr</i> : 1e-1